IEEE Access
Multidisciplinary | Rapid Review | Open Access Journal

Received March 4, 2018, accepted April 16, 2018, date of publication April 18, 2018, date of current version May 9, 2018.

Digital Object Identifier 10.1109/ACCESS.2018.2828325

The Predictive Functional Control and the Management of Constraints in GUANAY II Autonomous Underwater Vehicle Actuators

WILMAN ALONSO PINEDA MUÑOZ[1,2], (Member, IEEE), ALAIN GAUTHIER SELLIER[2], (Member, IEEE), AND SPARTACUS GOMÀRIZ CASTRO[3]

[1]Department of Electromechanical Engineering, GENTE Group, Universidad Pedagógica y Tecnológica de Colombia, Tunja 150462, Colombia
[2]Department of Electrical and Electronic Engineering, GIAP Group, Universidad de Los Andes, Bogotá 111711, Colombia
[3]Barcelona East School of Engineering, Electronic Engineering Department, Universitat Politécnica de Catalunya, BacelonaTech, 08019 Barcelona, Spain

Corresponding author: Wilman Alonso Pineda Muñoz (wilman.pineda@uptc.edu.co)

This work was supported in part Colciencias, Colombia

ABSTRACT Autonomous underwater vehicle control has been a topic of research in the last decades. The challenges addressed vary depending on each research group's interests. In this paper, we focus on the predictive functional control (PFC), which is a control strategy that is easy to understand, install, tune, and optimize. PFC is being developed and applied in industrial applications, such as distillation, reactors, and furnaces. This paper presents the first application of the PFC in autonomous underwater vehicles, as well as the simulation results of PFC, fuzzy, and gain scheduling controllers. Through simulations and navigation tests at sea, which successfully validate the performance of PFC strategy in motion control of autonomous underwater vehicles, PFC performance is compared with other control techniques such as fuzzy and gain scheduling control. The experimental tests presented here offer effective results concerning control objectives in high and intermediate levels of control. In high-level point, stabilization and path following scenarios are proven. In the intermediate levels, the results show that position and speed behaviors are improved using the PFC controller, which offers the smoothest behavior. The simulation depicting predictive functional control was the most effective regarding constraints management and control rate change in the Guanay II underwater vehicle actuator. The industry has not embraced the development of control theories for industrial systems because of the high investment in experts required to implement each technique successfully. However, this paper on the functional predictive control strategy evidences its easy implementation in several applications, making it a viable option for the industry given the short time needed to learn, implement, and operate, decreasing impact on the business and increasing immediacy.

INDEX TERMS Autonomous underwater vehicles, predictive functional control, management of constraints, high-level control, intermediate level control, TSK-Fuzzy, gain-schedulling, motion control, point stabilization, path following, industrial control systems.

I. INTRODUCTION

The motion control system of an autonomous underwater vehicle (AUV) consists of three blocks: the guidance, navigation, and control system as shown in Fig. 1. Since the end of the last decade to the present, various issues associated with each block have been addressed. The control system regulates the forces and moments required to satisfy a given control objective, which usually involves the guiding system. Some examples of control objectives are using minimum energy, tracking a set point, tracking or a variable trajectory over time, following predefined routes, and controlling maneuvers. Building a control algorithm involves designing anticipated and re-fed control laws. Outputs from the navigation system such as position, speed and acceleration are used by the feedback control, while feed forward control uses the available signals from the guidance system and other external sensors. A great variety of control techniques are used in autonomous underwater vehicles. The Italian

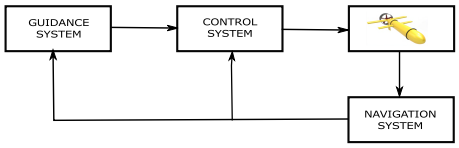

FIGURE 1. Blocks for control of movements of autonomous underwater vehicle.

vehicle, "Fogala", uses a combination of proportional integral derivate (PID) controllers with *backstepping* which demonstrates its effectiveness controlling immersion. In this project, careful adjustment of the parameters of the controller was made [1].

The *College of Automation* of *Harbin Engineering University* is one of the most prolific publishers on the design of controllers for submarine vehicles found in databases. One of its last works, presented in the magazine *Ocean Engineering* [2], integrates the PID control and *nonlinear sliding mode control* techniques to address trajectory tracking issues in an underwater vehicle using a model with parametric perturbations and constant unknown currents.

In the United Kingdom, Biggs and Holderbaum [3] formulate the motion issue as a problem of kinematical optimal control over a group of Euclidean movements, where the function of cost to be minimized is the quadratic integral of the velocity components. Ultimately, they demonstrate that a set of optimal movements traces helical paths.

Mohan and Kim from India and Korea, respectively, present an indirect adaptive control method using a Kalman filter in an AUV with a manipulator system. The design realized covers the disadvantages of the perturbations in the adaptive control observers schemes [4].

In [5], a group of researchers from the University of California and University of New York presented a method of minimizing course control time in an AUV with fixed. The authors report difficulties because of abounding local optimal trajectories; however, they find global optimal trajectories by solving the dynamic partial differential equation of Hamilton Jacobi Bellman. There is abundant information on the use of this optimization technique, which seeks to generate optimum paths in time [6]–[8].

Lapierre [9], from France, in pursuit of a solution to the problem of motion control that guarantees robustness in the presence of uncertain external parameters that make the dynamic model of the vehicle inaccurate proposed an immersion control based on Lyapunov theory and *backstepping* technique. However, Lapierre found internal instability issues produced by the noise induced in the evolution of some parameters, which impeded the implementation of the solution in an actual system.

There are studies addressing nonlinear controllers to stabilize AUV's susceptibility to uncertainties and current disturbance, as well as un-modeled dynamics and parameters variations [10], [11]. Rezazadegan *et al.* [12] propose an adaptive controller based on Lyapunov's direct method and back-stepping technique, which guarantees robustness against parameter uncertainties. Another significant work with adaptive nonsingular integral terminal sliding mode control was published by Qiao and Zhang [13].

At the University of Montpellier, Maaluof *et al.* [14] developed an adaptive control algorithm $\mathcal{L}_1$, for an autonomous underwater vehicle, which considers the nonlinearities of the dynamic system and variations of its parameters.

As for nonlinear control techniques, there are automatic pilots using the control in sliding modes. In 1993, Healey and Lienard [15] of Naval Postgraduate School of Monterrey published a study in which they tested heading, immersion and speed control. Sliding modes as variable structure control displayed robustness in complex maneuvers but is imprecision when the maneuvers involved tight turns. Another integral control in sliding modes was presented by the Pohan University of Science and Technology [16] to stabilize an AUV. The model proved robust and subject to unknown environmental disturbances.

The predictive model-based control (MPC) has also been used to control underwater vehicles. A group of researchers in underwater robotics from the School of Electrical and Electronic Engineering at the University of Sains, in Malaysia [17], analyzed the movement of a hybrid undersea glider with a predictive control with neural networks. They compared its performance with a predictive control based on model and a quadratic linear regulator. They also showed the glider's aerodynamic response to speed, the angle of attack and slip angle.

In [18] the robust predictive control (RMPC) is considered, and the nonlinear dynamics of the AUV with six degrees of freedom is linearized. This study uses linear models to represent the horizontal and vertical dynamics of the system.

Shen [19] presents a nonlinear model predictive control (NMPC) method for the trajectory problem of an autonomous underwater vehicle, several reference trajectories were tested, which demonstrate effectiveness and efficiency of the proposed algorithm.

In the United Kingdom, Sutton and his group [20] designed an automatic pilot using a genetic algorithm (*GA*) In line with a predictive controller based model. Despite the presence of perturbations and uncertainty in the model, the tests on the AUV carried out in real-time, showed a favorable performance of the control. The genetic algorithm was used as an optimization tool in the MPC, where the objective function was minimized *online* and subjected to soft and hard constraints on the actuators. The drawback encountered by Sutton and his team was the computational cost of using the GA, finding that implementation is not feasible for low sampling periods.

The studies found used genetic algorithms, neural networks and fuzzy logic for the control of AUVs. Genetic algorithms are used to adjust the parameters of the controllers. For example, in [21] GAs adjust linear quadratic regulator (LQR) parameters, and in [22], GAs adjust PID parameters, whereas in [23], GAs are used to find an optimal path. Neural networks

have been used to control the movement of AUVs [24] and as the basis of the model of the movement of the vehicles [25]. Advanced algorithms have been used to resolve issues concerning the control system; however, even these algorithms present drawbacks in the management of constraints in the actuators [26]–[28]. Predictive control algorithms stand out from others because they handle restrictions. The predictive functional control (PFC) is also prominent for its flexibility in the implementation phase [29]. The PFC has been successful in a significant number of industrial applications; however, it has not received enough attention in academic literature possibly because the predictive control community has been focused on other problems like stability [30]–[33], and working on algorithms implementation [34], [35].

Research on autonomous underwater vehicles predictive functional control is motivated, primarily, by the lack of adequate literature on the topic and the challenge other AUV control strategies have in managing actuators constraints. The design of AUV control schemes is challenging. The main difficulties include dynamic nonlinearities, complexities, and uncertainties, as well as unknown external disturbance. Different schemes have been evaluated to solve this AUV control issues. In [36], reference trajectories were generated by means of optimal control and tracked via nonlinear model predictive control; this approach satisfies the constraints imposed. To satisfy operation constraints, including time critical goals, kinematic modeling, and resource limitation, in [37], a model of environment constraints was proposed for autonomous robots in a cost and cognitive-based adaptive algorithm function. Although some noteworthy achievements were obtained in this studies, these controllers still require improvements in constraint management for practical applications.

In this document, through the application of a suboptimal practical solution, the predictive functional control demonstrates excellent performance handling constraints in the Guanay II autonomous underwater vehicle. The navigation tests of the Guanay II unmanned submarine were carried out on the Mediterranean Sea, these are agree with simulation result about movement of AUV.

The following section describes the hydrodynamic model, intermediate and high level controls, and PFC design for Guanay II. Subsequent sections explain the experimental results, and the last section presents the conclusions.

II. GUANAY II MOTION CONTROL

Motion control systems for marine craft is an active field of research. Modern control systems use techniques such as PID control, optimal control, neural networks and nonlinear control theory, to mention a few. Nonlinear control can often yield a more intuitive design than linear theory but the results can be a more complicated design process with limited physical inside.

The movement of autonomous underwater vehicles (AUV) is modeled in three hierarchical levels: high, intermediate, and low. In high-level control, the vehicle's control

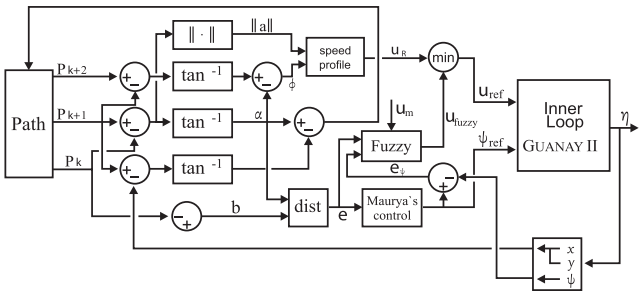

FIGURE 2. Block diagram: path following scenario.

scenarios and kinematic movement strategies are defined. In the intermediate level, the kinetic controls are defined, and in the low-level control, actuator control strategies are determined to optimize actuator constraints and management.

The high-level control or external loop of the Guanay II uses point stabilization and path following scenarios. The purpose of this control is to follow the reference or way-points defined by the mission to be fulfilled by the vehicle. The intermediate level control of Guanay II uses the TSK-Fuzzy, predictive functional, and gain-schedulling controls. The low-level control of the Guanay II uses a strategy to solve the optimization problem, which select the best option for the applied propulsion and torque of the thrusters. We design other optimal solution only when Guanay II uses PFC control.

The tests results obtained in the Mediterranean Sea demonstrate the excellent performance, in the intermediate level, of the PFC algorithm in controlling the longitudinal velocity of autonomous underwater vehicles and emphasize its easy implementation, as well as the efficient management of the restrictions on the actuators in the low level. We used ''path following'' and ''point stabilization'' scenarios in the high-level. In the intermediate level, we conducted simulations with gain-schedulling, TSK-fuzzy and PFC control. In real trials, we used TSK-Fuzzy and PFC control.

A. HIGH-LEVEL CONTROL: PATH FOLLOWING SCENARIO

In this case, the waitpoints must be close to each other. For yaw control, the Guanay II uses the Maurya Algorithm [38], which consist of a proportional-integral (PI) controller and a constraint with respect to the radius curvature. The velocity control algorithm is TSK-fuzzy controller, see Fig. 2. For our trials, we used a ''figure-eight'' pattern, see Fig. 3, near to the coast of Vilanova i la Geltru, in Barcelona.

B. HIGH-LEVEL CONTROL: POINT STABILIZATION SCENARIO

The position of the vehicle is input reference p_k. Velocity u_{ref}, and yaw ψ_{ref} are outputs of high-level control; they are also inputs of the intermediate level control or inner loop (Fig. 4). The objective of the hight-level control is to direct the vehicle towards the way-point and near this point with a defined curvature ratio. When the vehicle reaches this area,

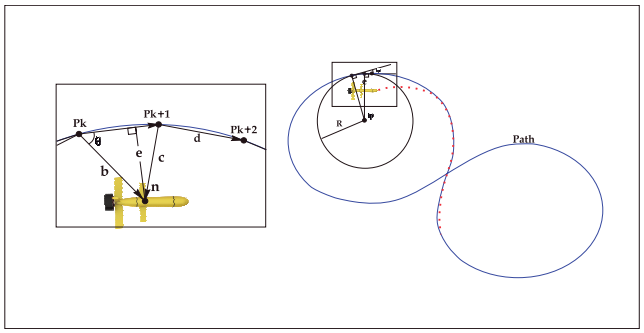

FIGURE 3. Path following in Guanay II.

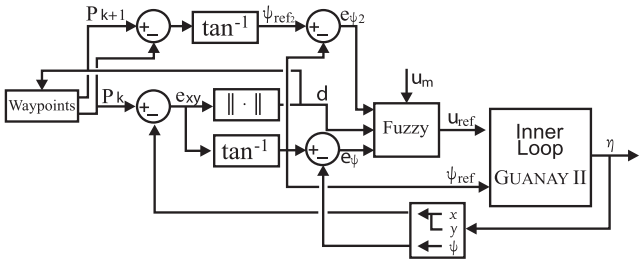

FIGURE 4. Block diagram: point stabilization scenario.

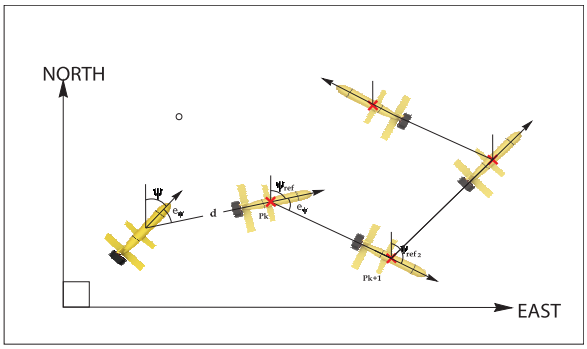

FIGURE 5. Point stabilization scenario.

it moves to another way-point until the mission is completed. The TSK-fuzzy control takes into account three parameters to establish the longitudinal reference velocity and the reference yaw for the intermediate level control. The parameters are the yaw error e_ψ, the distance between way-points d, and the angle that the vehicle must rotate upon reaching its target to find the next way-point ψ_{ref}. The parameters are shown in Fig. 5, where P_k is the current way-point and P_{k+1} is the next way-point.

C. INTERMEDIATE LEVEL CONTROL

The control of the dynamics of autonomous underwater vehicles is the intermediate control; in our case, it requires velocity and yaw reference signal inputs and applied outputs to manipulate variables *MV* on actuators. Guanay II was evaluated with different controls algorithms. First, in [39] funded by the Spain Ministry of Education and Science,

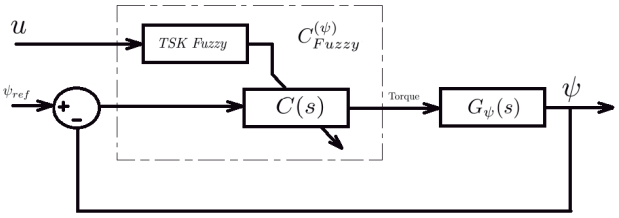

FIGURE 6. Bock diagram TSK-Fuzzy intermediate level control.

the FEDER Union. PID and TSK-fuzzy controllers were designed, compared and tested. PID controllers work well in specific zones of work; if the zone changes, the PID must change. The advantage of the TSK-fuzzy is the combination of PID options to address different work zones by using the best features for each zone. This is known as zonally differentiated control and uses piecewise lineal model. The results of this work were published in article [39], which underscore the advantages of TSK-fuzzy over PID controllers. In our work, we designed and tested PFC controllers and TSK-fuzzy controllers, and we compared simulation results and real test. Lastly, we simulated Gain Scheduling algorithm in order to obtain best analysis and conclusions. Thus far, PFC is so far the best control strategy in intermediate control for the Guanay II. Next, we present some information on the TSK-fuzzy and Gain Schedullin controls. Later, in section E, we present the PFC design.

1) INTERMEDIATE LEVEL CONTROL: TSK-FUZZY CONTROL

Takagi-Sugeno-Kang (TSK) is a method of fuzzy inference introduced in 1985. It is similar to the Mamdani method in many aspects. The first two parts of the fuzzy inference process, fuzzifying the inputs and applying the fuzzy operator, are the same. The main difference between Mamdani and Sugeno is that the Sugeno output membership functions are either linear or constant [40]. In the Guanay II vehicle, the parameters of $C(s)$ is dynamically modified by a fuzzy blocks; this control is represented as $C^{(\psi)}_{Fuzzy}$. $C(s)$ is PID controller. See Fig. 6. The same strategy is used for velocity control. More information on how many sets were used and how the sets were chosen is found in article [39].

2) INTERMEDIATE LEVEL CONTROL: GAIN SCHEDULING CONTROL

A gain scheduling controller is a controller whose gains are automatically adjusted as a function of time, operating condition, or plant parameters. In the Guanay II, the parameters of linear controllers are changed by longitudinal velocity. In Fig. 7. $C(S)$ is PID controller and $C^{(\psi)}_{GainsS}$ is yaw controller. Equation (1) shows polynomial regression that changes parameters $k_p^{(\psi)}(u)$ and $k_d^{(\psi)}(u)$.

$$k_p^{(\psi)}(u) = -106.78u^3 + 368.41u^2 + 42.748u + 311.96$$
$$k_d^{(\psi)}(u) = 60.85u^3 - 209.96u^2 - 24.36u + 417.13 \quad (1)$$

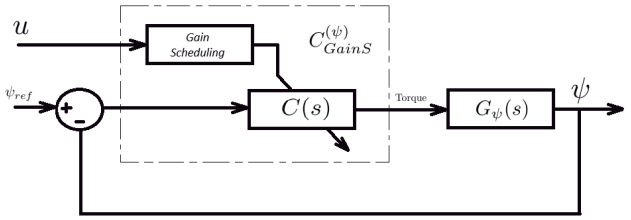

FIGURE 7. Block diagram: gain scheduling intermediate level control.

TABLE 1. Notation used in marine vehicles.

Description	Forces	Velocities	Positions
Motion in the x-direction (surge)	X	u	x
Motion in the y-direction (sway)	Y	v	y
Motion in the z-directions (heave)	Z	w	z
Rotation about x-axis (roll)	K	p	ϕ
Rotation about y-axis (pitch)	M	q	θ
Rotation about z-axis (yaw)	N	r	ψ

D. GUANAY II HYDRODYNAMIC MODEL

Starting with Fossen's vectorial model for marine vehicles [41], the model of Guanay II was obtained [42], [43]. Fossen's nonlinear equations, in the rigid body frame, can be written as:

$$\dot{\eta} = J_\Theta(\eta)\nu \tag{2}$$

$$(M_{RB} + M_A)\dot{\nu} + (C_{RB} + C_A)\nu + (D_n)\nu = \tau \tag{3}$$

where ν is the linear and angular velocities vector, τ is the generalized vector of external forces and momentums (see Table. 1). M_{RB} is the rigid body inertial matrix, M_A is the added mass matrix, C_{RB} is the rigid Coriolis and centripetal matrix, C_A is the hydrodynamics Coriolis and centripetal matrix, D_n is the hydrodynamic damping matrix. The total hydrodynamic damping can be written as the sum of components $D_P + D_S + D_W + D_M$. D_P is the radiation-induced potential damping due to forced body oscillations. D_S is the linear skin friction due to laminar boundary layers and quadratic skin friction due to turbulent boundary layers. D_W is wave damping, and D_M is damping due to vortex shedding (Morrison equation). Fossen represent the matrix D_p as the sum of the linear damping D_1 and nonlinear damping D_n.

Some matrices depend on coefficients expressed mathematically, such as the partial derivatives of the forces (X, Y, Z) or moments (K, M, N) with regards to a velocity or a position in the origin, so:

$$X_{\dot{u}} = \left.\frac{\partial X}{\partial \dot{u}}\right|_{\dot{u}=0}, X_u = \left.\frac{\partial X}{\partial u}\right|_{u=0}, X_{|u|u} = \left.\frac{\partial^2 X}{\partial u \partial |u|}\right|_{u=0}$$

According to the Nomenclature for Treating the Motion of a Submerged Body Through a Fluid [44] by The Society and Naval Architects and Marine Engineers, X, Y, Z represent the hydrodynamic force components relative to the body axes, referred to as longitudinal, lateral, and normal forces, respectively. K, M, N represent hydrodynamic momentums relative to the body axes, referred to as rolling, pitching, and yawing

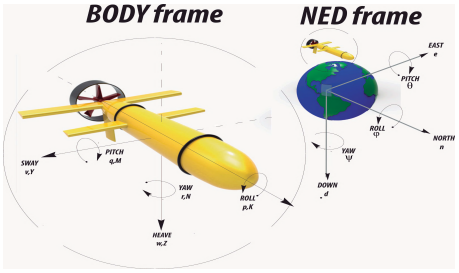

FIGURE 8. Body frame and north east and down NED frame.

TABLE 2. Hydrodynamic Coefficients for Guanay II.

$PARAMETER$	$VALUE$	$UNITS$
m	168.2000	Kg
I_z	52.7000	$Kg.m^2$
$X_{\dot{u}}$	-452.6809	Kg
$Y_{\dot{v}}$	-415.9546	Kg
$Y_{\dot{r}}$	-518.5884	$Kg.m/rad$
$N_{\dot{v}}$	18.3217	$Kg.m$
$N_{\dot{r}}$	-231.9244	$Kg.m^2/rad$
X_u	-0.2992	Kg/s
Y_v	-45.3418	Kg/s
Y_r	105.3055	$Kg.m/rad.s$
N_v	-3.3604	$Kg.m/s$
N_r	-56.9228	$Kg.m^2/rad.s$
$X_{\|u\|u}$	-152.6010	Kg/m
$Y_{\|v\|v}$	-399.4271	$Kg.m$
$Y_{\|r\|r}$	-899.5579	$Kg.m/rad^2$
$N_{\|v\|v}$	21.1978	Kg
$N_{\|r\|r}$	-284.1011	$Kg.m^2/rad^2$
c_{main}	0.0127	$Kg.m/s^2$
c_{lft}	0.0027	$Kg.m/s^2$
c_{rgt}	0.0029	$Kg.m/s^2$
a_{fin}	0.5000	m

movements, respectively. Regarding velocities, u, v, w are the components along the body axes of the linear velocity, and p, q, r are the components of the angular velocities vector relative to body axes x, y, z, referred to as angular velocities of roll, pitch, and yaw, respectively. The angle of elevation of the x-axis is θ known as the angle of pitch or trim, ψ is the angle of yaw and ϕ is the angle of roll (Fig. 8).

The Guanay II has been modeled with a velocity vector set as $\nu = [u, v, r]^T$. Consider the motion of the Guanay II represented by the following matrices and the hydrodynamic coefficients as in Table. 2, where these quantities are obtained by identification techniques [39].

$$M_{RB} = \begin{bmatrix} m & 0 & 0 \\ 0 & m & 0 \\ 0 & 0 & I_z \end{bmatrix} \tag{4a}$$

$$M_A = \begin{bmatrix} X_{\dot{u}} & 0 & 0 \\ 0 & Y_{\dot{v}} & Y_{\dot{r}} \\ 0 & N_{\dot{v}} & N_{\dot{r}} \end{bmatrix} \tag{4b}$$

$$C_{RB} = \begin{bmatrix} 0 & 0 & -mv \\ 0 & 0 & mu \\ mv & -mu & 0 \end{bmatrix} \tag{4c}$$

$$C_A = \begin{bmatrix} 0 & 0 & Y_{\dot{v}v} \\ 0 & 0 & -X_{\dot{u}u} \\ -(Y_{\dot{v}v} - Y_{\dot{r}r}) & X_{\dot{u}u} & 0 \end{bmatrix} \tag{4d}$$

$$D_1 = \begin{bmatrix} X_u & 0 & 0 \\ 0 & Y_v & Y_r \\ 0 & N_v & N_r \end{bmatrix} \tag{4e}$$

$$D_n = -\begin{bmatrix} X_{|u|u}|u| & 0 & 0 \\ 0 & Y_{|v|v}|v| & Y_{|r|r}|r| \\ 0 & N_{|v|v}|v| & N_{|r|r}|r| \end{bmatrix} \tag{4f}$$

where m is the mass of the vehicle, I_z is the vertical component of the inertial tensor. The forces and moments of Guanay II are represented by τ, as follows.

$$\tau = \begin{bmatrix} X \\ N \end{bmatrix} \tag{5}$$

$$X = X_{main} + X_{lft} + X_{rgt}$$

$$N = a_{fin} * (X_{lft} - X_{rgt}) \tag{6}$$

where X is the propulsion force, which moves the vehicle in the direction of the longitudinal velocity, N is the momentum in the z-axis relative to yawing, X_{main} represents the force applied by the main thruster, X_{lft} and X_{rgt} represent the forces applied by lateral thruster, and a_{fin} represents the distance from the lateral thruster to the longitudinal symmetrical axis of the vehicle. The following relations can be developed:

$$\begin{aligned} X_{main} &= c_{main} * \lambda_{main}|\lambda_{main}| \\ X_{lft} &= c_{lft} * \lambda_{lft}|\lambda_{lft}| \\ X_{rgt} &= c_{rgt} * \lambda_{rgt}|\lambda_{rgt}| \end{aligned} \tag{7}$$

Defining $\lambda_{main}, \lambda_{lft}, \lambda_{rgt}$ as the angular velocities normalized between the values -100 and 100 (as a percentage value) for the main thruster, left thruster, and right thruster, respectively.

To determine the linear equations of movements for Guanay II, it is assumed that the lateral velocity v and angular velocity r are negligible and the operation point is determined by the longitudinal velocity [39]. In this way, the transfer functions to the longitudinal velocity and yaw are expressed as:

$$G_u(s)_{u_0} = \frac{u(s)}{X(s)} = \frac{1}{(m - X_{\dot{u}})s - 2||u_0 X_{|u|u} - X_u} \tag{8}$$

$$G_\psi(s)_{u_0} = \frac{\psi(s)}{N(s)} = \frac{(m - Y_{\dot{v}})s - Y_v}{As^3 + Bs^2 + Cs} \tag{9}$$

where:

$$\begin{aligned} A &= (m - Y_{\dot{v}})(I_z - N_{\dot{r}}) - Y_{\dot{r}}N_{\dot{v}} \\ B &= (m - X_{\dot{u}})(N_{\dot{v}} - Y_{\dot{r}})u_0 - (m - Y_{\dot{v}})N_r \\ &\quad - (I_z - N_{\dot{r}})Y_v - Y_{\dot{r}}N_v - N_{\dot{v}}Y_r \\ C &= Y_v(Y_{\dot{r}}u_0 + N_r) + ((Y_{\dot{v}} - X_{\dot{u}})u_0 + N_v)((m - X_{\dot{u}})u_0 - Y_r) \end{aligned}$$

The subscript u_0 represents the operational point where the model is linearized.

Guanay II AUV is a highly nonlinear system. If we design a linear control around a specific velocity u_0, performance will be optimal approaching this velocity but not at other velocities. The Guanay II has two operational or works points at 0.3 m/s and 2 m/s, respectively and the nonlinear model is approximated by piecewise lineal model. Consequently, the transfer functions, in accordance with these points, can be obtained.

$$G_\psi(s)_{0.3} = \frac{0.003323s + 0.000258}{s^3 + 0.8107s^2 + 0.05834s} \tag{10}$$

$$G_\psi(s)_{2.0} = \frac{0.003323s + 0.000258}{s^3 + 4.0350s^2 + 0.7354s} \tag{11}$$

$$G_u(s)_{0.3} = \frac{0.001611}{s + 0.148} \tag{12}$$

$$G_u(s)_{2.0} = \frac{0.001611}{s + 0.9836} \tag{13}$$

$G_u(s)$ is the transfer function that relates the Laplace transform of longitudinal velocity u to hydrodynamic force X. $G_\psi(s)$ is the transfer function that relates the Laplace transform of yaw ψ to the hydrodynamic momentum on yaw N.

E. INTERMEDIATE LEVEL CONTROL: PREDICTIVE FUNCTIONAL CONTROL PFC DESIGN

Some decades of industrial practice with nonlinear systems and Predictive Functional Control algorithms have reported, in the archival literature, on distillation [45], reactors [46], and furnaces [47], among others. We are the first to demonstrate a PFC algorithm on autonomous underwater vehicles.

The algorithms implemented in Guanay II are PID, Gain Scheduling TSK-Fuzzy and PFC controls. The control objective by high-level control is the tracking reference of velocity and yawing. To date, the Takagi-Sugeno-Kang (TSK) fuzzy controller has been the best strategy for the Guanay II [39]. However, an optimization problem must be solved for the management of actuator constraints. The Predictive Functional Controller design presented in this document resolves constraints issues directly.

According to Richalet [29], Predictive Functional Control takes into account the following fundamental concepts:

- Internal model.
- Reference trajectory.
- Manipulated variable computing.

The hydrodynamic model of Guanay II is described by (4a),(4b),(4f),(4e), (4c), (4d). The reference trajectory sets the temporal path to be followed to reach the reference point; therefore, the reference trajectory sets the closed-loop dynamic of the control system and updates it at each new sample point, see Fig.9. The choice of function to be implemented is open; it can be a look-up table, calculated analytically, or it may depend on the time or state of the process (e.g tracking error). Then, an objective searches for an upcoming action so that the next response agrees with some fixed points on the reference trajectory, which are referred to as coincidence points. We choose one point as the coincidence point in $(k + H)$ and a reference trajectory exponential for the Guanay II for several reasons. First, only one point is used during initialization, in this case, the last measured output value. Second, the function is easy to calculate in real time. Lastly,

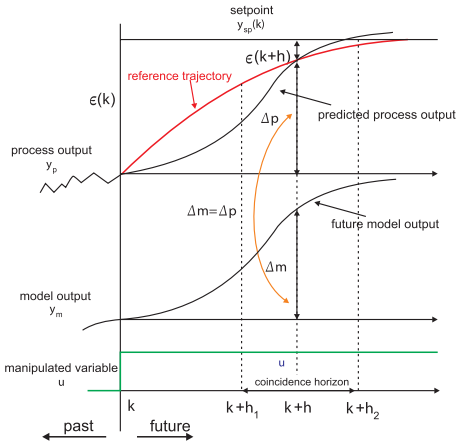

FIGURE 9. Reference trajectory with PFC control.

its decrement occurs predictably.

$$y(k) = \exp^{\frac{-kT_S}{T}} \tag{14}$$

where the decrement is:

$$\lambda = \exp^{\frac{-T_S}{T}} \tag{15}$$

and the sample time is Ts.

The regulation error, i.e., the difference between the *set point* and the process output in k is $e(K)$ and in $(k + H)$, the predicted error is given by $e(k + H) = \lambda^H * e(k)$. The output desired increment of y_p in $(k + H)$ is:

$$\Delta_p = \epsilon(k + h) = \epsilon(k) \tag{16}$$

where:

$$\Delta_p = -\epsilon(k)\lambda^H + \epsilon(k) = \epsilon(k)(1 - \lambda^H) \tag{17}$$

Finally:

$$\Delta_p = (Setpoint - Processoutput(k))(1 - \lambda^H) \tag{18}$$

The output increment desired Δ_p is obtained by measuring the output process and the reference signal; therefore, it is known as the reference trajectory. the manipulated variable must be assessed based on the plant mathematical model. The control signal will produce an increment in the output model Δ_m equal to Δ_p. So, the control is incremental, and can be given as:

$$\Delta_p = \Delta_m \tag{19}$$

If the plant model is known, it is possible to select the best manipulate variable using simulation test. The control signal should near to the desired increment while following the reference trajectory as closely as possible. Manipulated variables should be structured around the *basis functions* according to the nature of the variables and control, and the calculation complexity. The vector of future manipulated variables is not established directly. Instead, it is determined by the projection μ_j of manipulated variables MV on a finite set of basics functions:

$$F_j(i) = MV(k + i) = \sum \mu_j F_j(i) \tag{20}$$

where $j = 0, 1, , N - 1$ and $0 <= i <= H$. Thus, the manipulated variables are presented as a weighted sum of a finite number of N basis function. Namely, the cases in which each function consists of a polynomial base is referred to as Predictive Functional Control. The Guanay II uses the elemental case in velocity control, where $H = 1$, $F_0 = i^0 = 1$. Therefore, $u(k + 1) = u(k)$.

The following section explains, without loss of generality, the PFC design for first order models [48]. Proper models in high order can be classified into first order models. This favors the design of composite controllers based on a collection of controllers of first order PFC [49], [50].

1) THE FIRST ORDER PROCESS

For a first order system such as the longitudinal velocity control in the Guanay II, 95 percent of the response parallels with its time constant with relation to $3 * \tau$. As a result, the closed loop time response (CLRT) is three times the time constant of the system τ. The first order process takes the form of:

$$G(s) = \frac{Km}{1 + \tau s} \tag{21}$$

If we define $a_m = e^{\frac{T_s}{\tau}}$, as the difference equation that describes a process of first order without delay with a sample time T_s, and one time constant τ is given by:

$$y_m(k) = y_m(k - 1)a_m + (1 - a_m)K_m MV(k - 1) \tag{22}$$

The future output $y_m(k + H)$ to model is the sum of the free output response and the forced output response.

$$\begin{aligned} freeoutput(k + H) &= y_m(k)a_m^H \\ forcedoutput(k + H) &= MV(k)K_m(1 - a_m^H) \end{aligned} \tag{23}$$

The model increment in $(k + H)$ is given by

$$\Delta_m = y_m(k + H) - y_m(k) \tag{24}$$

and, therefore, the following is obtained:

$$\begin{aligned} \Delta_m &= freeoutput(k + H) \\ &\quad + forcedoutput(k + H) - y_m(k) \\ \Delta_m &= y_m(k)a_m^H + MV(k)K_m(1 - a_m^H) - y_m(k) \end{aligned} \tag{25}$$

The objective $\Delta_m = \Delta_p$ is met, so

$$\begin{aligned} &(Setpoint - y_p(k))(1 - \lambda^H) \\ &\quad = y_m(k)a_m^H + MV(k)K_m(1 - a_m^H) - y_m(k) \end{aligned} \tag{26}$$

By isolating the manipulated variable, the control law is obtained:

$$\begin{aligned} MV(k) = &\frac{(Setpoint - y_p(k))(1 - \lambda^H)}{K_m(1 - a_m^H)} \\ &- \frac{y_m(k)a_m^H + y_m(k)}{K_m(1 - a_m^H)} \end{aligned} \tag{27}$$

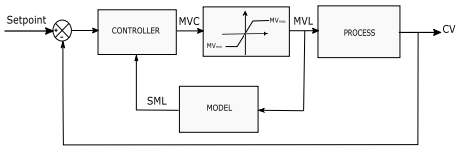

FIGURE 10. The inclusion of constraints in predictive functional control.

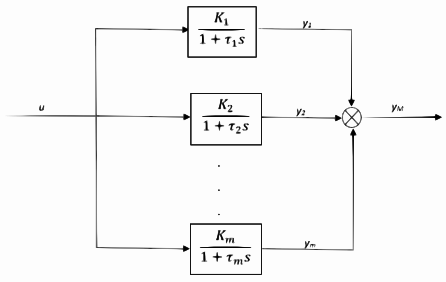

FIGURE 11. Internal model in parallel form.

On the other hand, the less common level constraints are taken into account in PFC. So MV_{max}, MV_{min}, D_{max} and D_{min} are taken into account.

$$MV_{min} < MV(k) < MV_{max} \tag{28}$$

and

$$D_{min} < MV(k) - MV(k-1) < D_{max} \tag{29}$$

In Fig. 10 the MVC calculated by the regulator R is passed initially through a speed limiter followed by an amplitude limiter. The resulting value $MVL(n)$ is then supplied as the input to the internal model of the regulator that, in turn, produces the model output SML.

2) HIGHER ORDER PROCESS

In the case of higher order process such as the yaw control on the Guanay II, the transfer function can be expressed as a decomposition in parallel or cascade [49], [50] in order to simplify the PFC design. The yaw control for the Guanay II uses parallel decomposition (Fig. 11), as represented by:

$$G_m(s) = \sum_{i=1}^{m} \frac{K_i}{1+\tau_i s}$$

From Fig. 11 the model output is given by:

$$y_M(k) = y_1(k) + y_2(k) + \ldots + y_m(k) = \sum_{i=1}^{m} y_i(k) \tag{30}$$

The difference equation equivalent of model in (30) is given by:

$$y_i(k) = \alpha_i y_i(k-1) + K_i(1-\alpha)u(k-1) \quad 1 \le i \le m \tag{31}$$

where $\alpha_i = e^{-(\frac{T_s}{\tau_i})}$, with T_s as sampling period. Replacing 31 into 30 we obtained model output:

$$\begin{aligned} y_M(k) &= \alpha_1 y_1(k-1) + \alpha_2 y_2(k-1) \\ &\quad + \ldots \alpha_m y_m(k-1) + [K_1(1-\alpha_1) + K_2(1-\alpha_2) \\ &\quad + \ldots + K_m(1-\alpha_m)] * u(k-1) \end{aligned} \tag{32}$$

Therefore,

$$y_M(k) = \sum_{i=1}^{m} \alpha_i y_i(k-i) + \sum_{i=1}^{m} K_i(1-\alpha_i)u(k-1) \tag{33}$$

The output model $y_M(k+H)$ may be divided in free $y_{M_{free}}(k+H)$ and forced $y_{M_{forced}}(k+H)$ response, so:

$$y_{M_{free}}(k+H) = \sum_{i=1}^{m} \alpha_i^H y_i(k) \tag{34}$$

$$y_{M_{foced}}(k+H) = \sum_{i=1}^{m} K_i(1-\alpha_i^H)u(k) \tag{35}$$

The reference trajectory $y_R(k)$ used in PFC is generally in an exponential form, and it is given by function of the $Setpoint(k)$ and the process output $y_p(k)$ as

$$y_R(k+H) = Setpoint(k) - \ldots \lambda^H(Setpoint(k) - Y_p(k)) \tag{36}$$

where $\lambda = e^{-(\frac{T_s}{T_R})}$ with T_R is Closed Loop Response Time (CLRT) and T_s the sampling time.
The process output estimated at time $k+H$ is given by:

$$\begin{aligned} \widehat{y}_p(k+H) &= y_M(k+H) + (y_p(k) - y_M(k)) \\ \widehat{y}_p(k+H) &= \sum_{i=1}^{m} y_i(k+H) + (y_p(k) - \sum_{i=1}^{m} y_i(k)) \end{aligned} \tag{37}$$

At coincidence point H the estimated process output $\widehat{y}_p$ is equal to the reference trajectory. Then

$$\begin{aligned} y_R(k+H) &= \widehat{y}_p(k+H)Setpoint(k) \\ &\quad -\ldots\lambda^H(Setpoint(k) - y_p(k)) \\ &= y_M(k+H) - y_M(k) \end{aligned} \tag{38}$$

Agreeing with (11), (34) and (35), if you use a step input basis function, see (20), we can write next equations.

$$\begin{aligned} &(1-\lambda^H)(Setpoint(k) - y(k) \\ &\quad = y_{M_{free}}(k+H) + y_{M_{foced}}(k+H) - \sum_{i=1}^{m} y_i(k) \\ &(1-\lambda^H)(Setpoint(k) - y(k) \\ &\quad = \sum_{i=1}^{m} \alpha_i^H y_i(k) + \sum_{i=1}^{m} K_i(1-\alpha_i^H)u(k) - \sum_{i=1}^{m} y_i(k) \\ &(1-\lambda^H)(Setpoint(k) - y(k) \\ &\quad = \sum_{i=1}^{m} K_i(1-\alpha_i^H)u(k) - \sum_{i=1}^{m} y_i(k) - \alpha_i^H y_i(k) \end{aligned}$$

$$(1-\lambda^H)(Setpoint(k)-y(k) = \sum_{i=1}^{m} K_i(1-\alpha_i^H)u(k) - \sum_{i=1}^{m}(1-\alpha_i^H)y_i(k) \quad (39)$$

$$u(k) = MV(k) = \frac{(Setpoint - y_p(k))(1-\lambda^H)}{\sum_{i=1}^{m} K_i(1-\alpha_i^H)} + \ldots \frac{\sum_{i=1}^{m} y_i(k)(1-\alpha_i^H)}{\sum_{i=1}^{m} K_i(1-\alpha_i^H)} \quad (40)$$

where $MV(k)$ is manipulated variable. The constraints are managed as in first order systems. The constraints are managed as in first-order systems.

3) GUANAY II PFC

Although the Guanay II model, given to equations (10), (11),(12), and (13) is piecewise lineal model, when we designed the PFC controller, we took into account only one work point on the velocity and another on the yaw. Therefore, we selected the model provided by (10) and (12). PCF differs from traditional predictive controllers. Because of its incremental characteristic, a highly precise model is not required.

The PFC's incremental characteristic means that the model changes each sampled time. The model and the process are assumed to have the same qualitative structure. Prior values of the model and process are known through sensors and the manipulated variable MV that delivers the increment Δm, see equations (19),(24), and (25). This technique can guarantee the stability and robustness of control system.

The discrete time model for yaw $G\psi(z)$ and longitudinal velocity $G_u(z)$ is obtained with a sample time T_s equal to 0.1 s. In a discrete time control system, the control input is assumed constant during the sample interval. The sample time for the Guanay II satisfies system dynamic and bandwidth requirements in agreement with a Niquist-Shanoon sampling Theorem. The discrete (41) on the Guanay II is the Z-transform of (10); the discrete (42) is the Z-transform of (12); and, (43), (44) and (45) are partial fractions taken from (42).

$$G_u(z) = \frac{0.0001599}{z-0.9853} \quad (41)$$

The parallel decomposition is:

$$G\psi(z) = \sum_{i=1}^{3} G_{\psi_i}(z) \quad (42)$$

$$G_{\psi_1} = \frac{-0.0004399}{z-0.9295} \quad (43)$$

$$G_{\psi_2} = \frac{-1.389 * 10^{-5}}{z-0.9295} \quad (44)$$

$$G_{\psi_3} = \frac{0.0004422}{z-1} \quad (45)$$

The discrete control law for longitudinal velocity in terms of propulsion is obtained by the method explained above for first order systems. See (27).

$$MV(k) = X(k) \quad (46)$$

$$X(k) = \frac{(u_{setpoint} - u_p(k))(1-\lambda_1^H)}{K_m(1-a_m^H)} - \frac{u(k)a_m^H + u(k)}{K_m(1-a_m^H)} \quad (47)$$

where $X(k)$ is the propulsion in the engines, $u_p(k)$ and $u(k)$ are longitudinal velocities given by the sensors and the model, respectively. The $u_{setpoint}$ is set by the guidance system on high-level control.

The discrete control law for the yaw position in terms of momentum in the z-axis relative to yawing is obtained using the method referred to above for high order systems. See (40).

$$MV(k) = N(k) \quad (48)$$

$$N(k) = \frac{(\psi_{setpoint} - \psi_p(k))(1-\lambda_2^H)}{\sum_{i=1}^{m} K_i(1-\alpha_i^H)} + \frac{\sum_{i=1}^{m} \psi_i(k)(1-\alpha_i^H)}{\sum_{i=1}^{m} K_i(1-\alpha_i^H)} \quad (49)$$

where $N(k)$ is the moment in the z-axis relative to yawing, $\psi(k)$ is the yaw movement given by the compass, and ψ_i is given by the model. The $\psi_{setpoint}$ is given by the guidance system on high-level control.

The adjustment parameters from PFC are the coincidence point "H" and the decrement "λ". The Guanay II uses $H = 1$ and $\lambda_1 = 0.75$ for the longitudinal velocity. The parameters for yaw control are $H = 20$ and $\lambda_2 = 0.9$. In [49] and [50] there are techniques for adjusting parameters in high order systems.

III. SIMULATIONS RESULTS

In the case of nonlinear systems there is no general theory governing the real application to nonlinear processes. Thus, the discussion will be limited to the treatment of some specific cases. If the process state is known, by measurement or estimation, it is feasible to create a scenario with the aid of the model. Using an adequate method with a nonlinear solver, the manipulated variable MV scenario describing the evolution of the model output toward the specific point on the reference trajectory can be calculated. In our case, the process is locally differentiable without singularities, a local projection is used that changes at each instant. However, the solution may be improved by using a classical method for solving nonlinear algebraic equations such as the Raphson-Newton method, which improves the accuracy of the control equation.

PFC industrial implementations with nonlinear models are possible. In [51], a PFC control was implemented in the Yokogawa CS3000 integrated production control system. In [52],

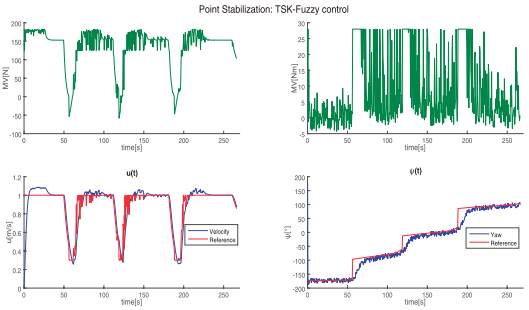

FIGURE 12. On the right, *MV* and longitudinal velocity of vehicle. On the left, *MV* and yawing position of the vehicle.

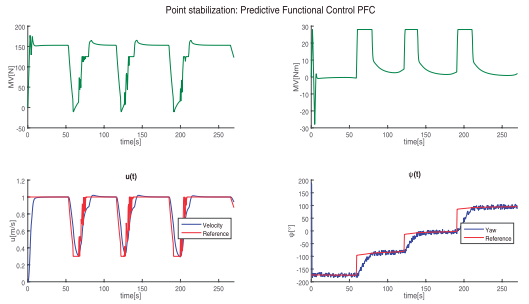

FIGURE 13. On the right, *MV* and longitudinal velocity of vehicle. On the left, *MV* and yawing position of the vehicle.

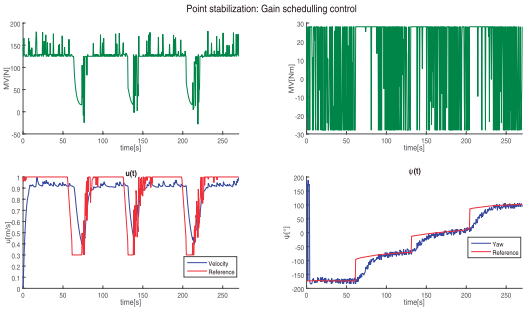

FIGURE 14. On the right,*MV* and longitudinal velocity of vehicle. On the left, *MV* and yawing position of the vehicle.

PFC was applied to temperature control system of an electric heating furnace. These experiments demonstrate the validity and effectiveness of the control algorithm. Reference [53] describes three industrial applications of PFC for two distillation columns and a reactor in a petrochemical plant.

PFC design control on Guanay II is calculated with a piecewise lineal model on a work point 0.3 m/s, but was proven with 0.6 m/s and 1 m/s, see figures 25 and 26. This is a practical demonstration on the excellent performance of the incremental model, working in different work points. Lastly, in Barcelona, Guanay II vehicle was tested in open-sea where it was subject to uncertainty and disruption, demonstrating the PFC's robustness.

The manipulated variable *MV* obtained from piecewise lineal model was applied to nonlinear model, given by equations (4) for simulation, and finally is programmed on

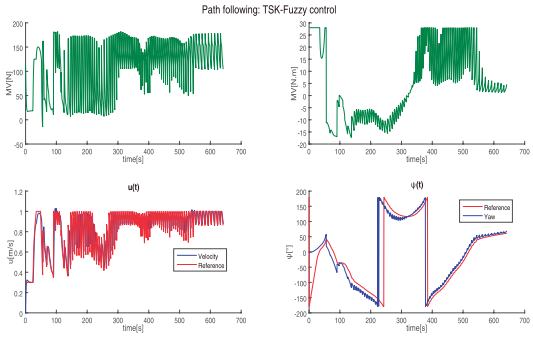

FIGURE 15. On the right, *MV* and longitudinal velocity of vehicle. On the left, *MV* and yawing position of the vehicle.

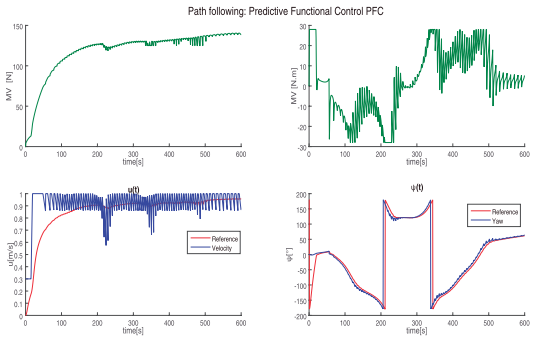

FIGURE 16. On the right, *MV* and the longitudinal velocity of vehicle. On the left, *MV* and yawing position of the vehicle.

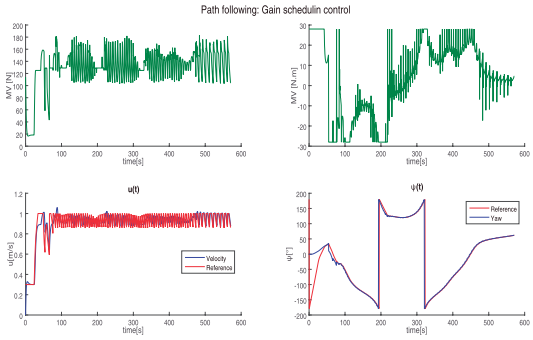

FIGURE 17. On the right, *MV* and longitudinal velocity of vehicle. On the left, *MV* and yawing position of the vehicle.

electronic board, and applied to real vehicle in order to obtain our real test results.

Three control strategies and two control scenarios for the Guanay II movement were simulated to analyze the behavior of intermediate level controls. Fig. 12, Fig. 13 and Fig. 14 show the behavior of TSK-Fuzzy, PFC and Gain Scheduling controls with *point stabilization* scenario. Fig. 15, Fig. 16 and Fig. 17 shows the TSK-Fuzzy, PFC and Gain Scheduling controls with *path following* scenario.

The manipulated variable *MV* activates the engines of the Guanay II generating the propulsion that controls the longitudinal speed of the vehicle and its hydrodynamic moment relative to the yawing movement on the z-axis.

TABLE 3. Characteristics of the tests carried out.

	Maximum velocity m/s	Control Scenario	Controller
Test 1	0.6	Point Stabilization	PFC
Test 2	0.6	Point Stabilization	PFC
Test 4	0.6	Point Stabilization	TSK-Fuzzy
Test 5	0.6	Path Following	PFC
Test 7	0.6	Path Following	TSK-Fuzzy
Test 8	1	Path Following	PFC
Test 9	1	Path Following	TSK-Fuzzy

TABLE 4. Geographic coordinates for point stabilization.

	Longitude	Latitude
way-point 1	$41°12'32.85''$	$1°43'27.43''$
way-point 2	$41°12'32.85''$	$1°43'24.50''$
way-point 3	$41°12'30.95''$	$1°43'24.84''$
way-point 4	$41°12'30.98''$	$1°43'27.14''$

FIGURE 18. Way-points on point stabilization scenario. Barcelona coast in the Mediterranean Sea.

According to the control scenario defined by the vehicle mission, the objective of high-level control may be to follow a path or visit a set of specific way-points. The high-level control give yawing and velocity references to intermediate level control. The intermediate level control following reference and generate manipulated variables *MV* for applied on thrusters.

The curves in all simulation results show that, in all cases, the objectives of intermediate level controls are adequately fulfilled. However, the behavior of manipulated variable *MV*, in the case of the intermediate level control, strategy of the predictive functional control (PFC) should be emphasized. As can be seen in Fig. 13 and Fig. 16 the signal does not present changes or oscillations compared to the other controls. The soft behavior of *MV* in PFC's protects the actuators and extends their useful life compared to another control strategies.

IV. EXPERIMENTAL RESULTS IN MEDITERRANEAN SEA

Nine test were conducted with the Guanay II in the coast of Barcelona in Mediterranean Sea to verify the results of the simulations using the predictive functional control (PFC), see Table. 3. The first four tests were performed using the *point stabilization* scenario; the last five use *path following* of the high-level control scenario. TSK-fuzzy and PFC controls were used for intermediate level of control tests to test the advantage of using PFC, considering that in previous works,

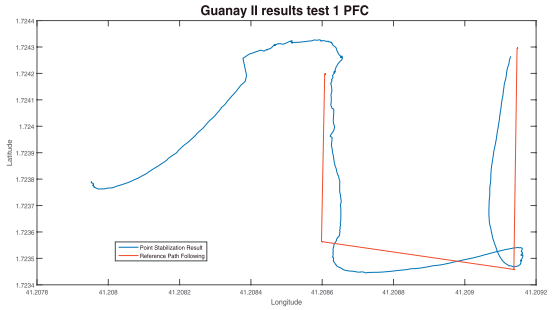

FIGURE 19. Test 1- Point stabilization scenario with PFC.

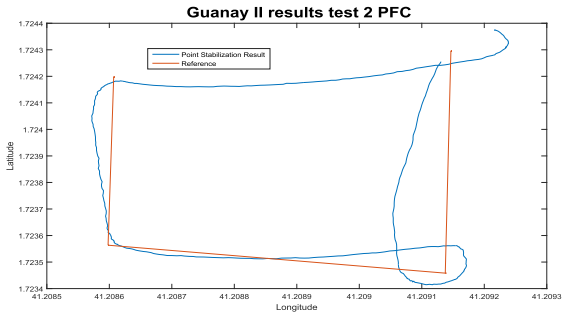

FIGURE 20. Test 2-Point stabilization with PFC.

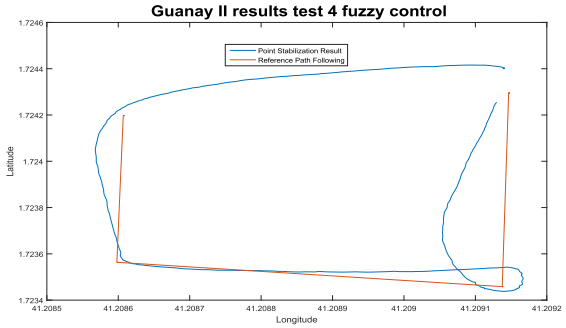

FIGURE 21. Test 4-Point stabilization with TSK-Fuzzy.

the TSK-fuzzy was the best control strategy compared to other linear and nonlinear strategies such as gain scheduling control. These controls are the same as those used in simulation results.

In actual trials, the Guanay II fulfilled the objectives proposed for each mission. The vehicle reached the four way-points established in the point stabilization scenario, see Figure 20. The Guanay II also followed the 8-path determined for the path following scenario as shown Figure 25.

The predictive functional control (PFC) is set with two parameters, the coincidence point H and the decrement λ. PFC is the predictive controller used to control the movements of the Guanay II; it includes speed and yaw controls. For forward speed $\lambda = 0.65$ and $H = 1$, yaw control $\lambda = 0.65$ and $H = 20$. The previous given that the transfer function of the forward speed is of the first order, while the yaw transfer function is of the third order. We were certain of the behavior of the PFC in first order systems but were unsure

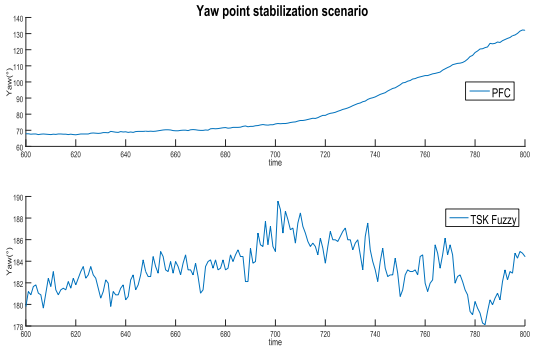

FIGURE 22. Point Stabilization scenario: Yaw position with PFC and TSK-fuzzy controllers.

FIGURE 23. Path following Scenario. Barcelona coast in the Mediterranean Sea.

TABLE 5. Way-points over path following scenario.

	Longitud	Latitud
way-point 0	$41°12'31.56''$	$1°43'26.13''$
way-point 1	$41°12'32.89''$	$1°43'29.94''$
way-point 2	$41°12'31.58''$	$1°43'22,73''$
way-point 3	$41°12'30.36''$	$1°43'24.18''$
way-point 4	$41°12'28.98''$	$1°43'26.09''$
way-point 5	$41°12'28.55''$	$1°43'22.60''$
way-point 6	$41°12'27.67''$	$1°43'24.11''$

in the case of systems of orders greater than one. Information on the PFC control technique can be found in [27], [29], [49], and [50].

In the first seven tests, the vehicle was set to a maximum speed was of 0.6 m/s. In the last two tests, the maximum speed was increased to 1 m/s. It should be noted that the reference speed is determined by the high-level control; when the speed is set to a maximum value, the vehicle travels at speeds inferior to this value. The data acquisition system of the Guanay II provided the information to obtain the graphs presented.

A. RESULTS WITH POINT STABILIZATION SCENARIO

The Guanay II underwater vehicle initiated its autonomous operation in a length of $41°12'28.63''$ to the east and a latitude $1°43'25,65''$ to the north. Maritime coordinates of points are shown in table 4 and the route followed is in Fig. 18.

Fig. 19 shows how the vehicle is systematically directed to each way-point. Test one is repeated so that each test had the same trajectory starting point, thus allowing the comparisons between all the controls. The results of these test are in Fig. 20. The TSK-Fuzzy control was used in Fig. 21. Experimental results the point stabilization scenario show a soft behavior when we used PFC control in intermediate level. See Fig. 22.

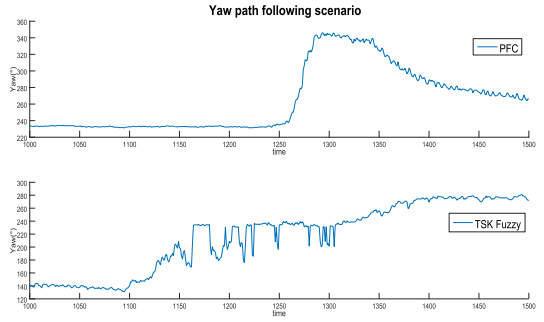

FIGURE 24. Path following scenario: Yaw movement with PFC and TSK-fuzzy controllers.

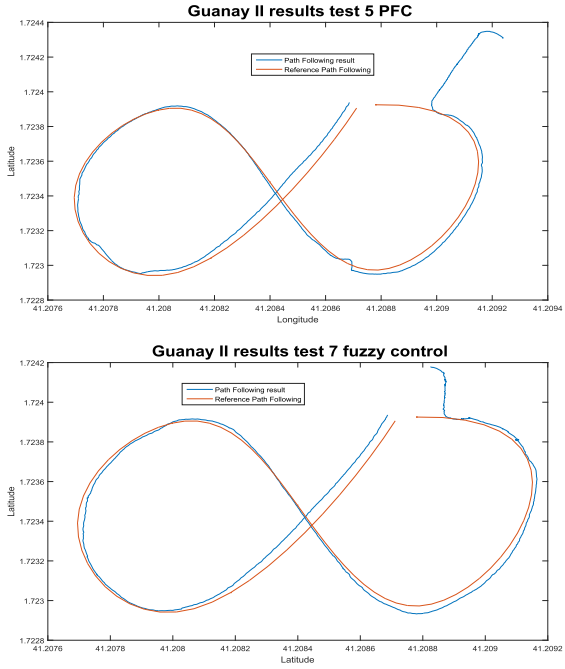

FIGURE 25. Test 5 an 7. Path Following with PFC and TSK-Fuzzy. Longitudinal velocity 0, 6 m/s.

B. RESULTS WITH PATH FOLLOWING SCENARIO

Figure 23 presents the routes of the path following scenario. Table. 5 presents some of the points on the routes to provide an idea of maritime location where the tests were carried out. Again, predictive functional control and TSK-Fuzzy were tested. The results are presented in Figure 25. The longitudinal velocity was increased from $0,6$ m/s to 1 m/s in the last two trials. The results using PFC and TSK-Fuzzy controllers are show in Figure 26. Experimental results the path following scenario show a soft behavior when we used PFC control in intermediate- level. See figure 24.

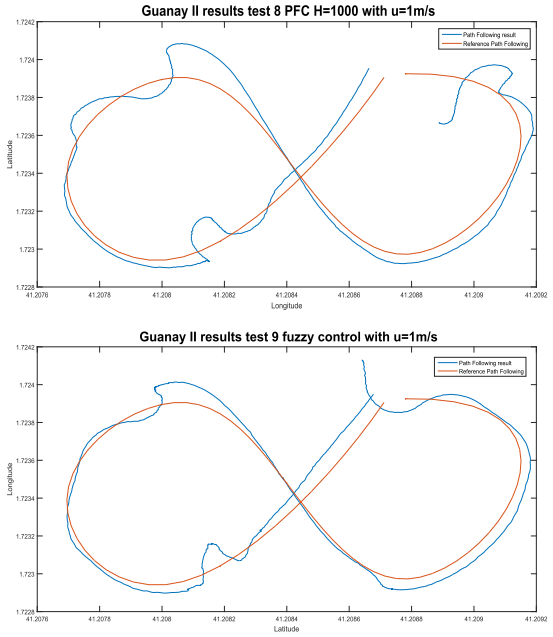

FIGURE 26. Test 8 and 9. Path Following with PFC and TSK-Fuzzy. Longitudinal velocity 1 m/s.

V. CONCLUSION

The results show that the TSK-fuzzy control and predictive functional control (PFC) strategies meet the objectives outlined in each movement control scenario. However, the PFC stands out for its performance in the ''manipulated variable'' *MV* signal. The behavior of the ''manipulate variable'' *MV* protects the thrusters by preventing sudden changes in the control; this extends the useful life of the thrusters. The results obtained in the simulations have been verified by real navigation test in the Mediterranean Sea. The predictive functional control has been tested in multiple industrial applications. This investigative work demonstrates that control of underwater vehicles can also be used. Numerous academic works have contributed to the theoretical development of the PFC, making it a prolific field of research for those interested in the industrial control sciences. The characteristics of PFC can be programmed easily into Guanay's embedded systems. The predictive functional control is robust because it take into account disturbances and the variations of model parameters; its incremental characteristic allow it to adjust constantly, see (19).

If the coincidence horizon is short, the *MV* is strong, but the predicted response is close to the reference trajectory. If the coincidence horizon is long, the *MV* is less vigorous but the velocity and yaw differ from the reference trajectory. The constraint on the *MV* does not have to be applied rigorously but may be voluntarily relaxed to protect the process from excessive actions; furthermore, it is easy to implement.

Taking constraints into account is a key concerning control when optimizing efficiency by maximizing the available power of the actuators. Handling constraints in the ''manipulate variable'' *MV* is a straightforward procedure with PFC.

The PFC control signal does not have oscillation when faced with sensor noise, while others strategies show oscillations in this situation.

The predictive functional control perform adequately in SISO simple input and output systems. A topic for future investigations is its use in MIMO multiple input and output systems, as the PFC's designs and implementation philosophy should be simple and flexible.

REFERENCES

[1] A. Alvarez *et al.*, ''Fòlaga: A low-cost autonomous underwater vehicle combining glider and AUV capabilities,'' *Ocean Eng.*, vol. 36, no. 1, pp. 24–38, Jan. 2009.
[2] Z. Yan, H. Yu, W. Zhang, B. Li, and J. Zhou, ''Globally finite-time stable tracking control of underactuated UUVs,'' *Ocean Eng.*, vol. 107, pp. 132–146, Oct. 2015.
[3] J. Biggs and W. Holderbaum, ''Optimal kinematic control of an autonomous underwater vehicle,'' *IEEE Trans. Autom. Control*, vol. 54, no. 7, pp. 1623–1626, Jul. 2009.
[4] S. Mohan and J. Kim, ''Indirect adaptive control of an autonomous underwater vehicle-manipulator system for underwater manipulation tasks,'' *Ocean Eng.*, vol. 54, pp. 233–243, Nov. 2012.
[5] B. Rhoads, I. Mezić, and A. C. Poje, ''Minimum time heading control of underpowered vehicles in time-varying ocean currents,'' *Ocean Eng.*, vol. 66, pp. 12–31, Jul. 2013.
[6] M. Ataei and A. Yousefi-Koma, ''Three-dimensional optimal path planning for waypoint guidance of an autonomous underwater vehicle,'' *Robot. Auto. Syst.*, vol. 67, pp. 23–32, May 2015.
[7] Y. Li, C. Wei, Q. Wu, P. Chen, Y. Jiang, and Y. Li, ''Study of 3 dimension trajectory tracking of underactuated autonomous underwater vehicle,'' *Ocean Eng.*, vol. 105, pp. 270–274, Sep. 2015.
[8] K. Mukherjee, I. N. Kar, and R. K. P. Bhatt, ''Region tracking based control of an autonomous underwater vehicle with input delay,'' *Ocean Eng.*, vol. 99, pp. 107–114, May 2015.
[9] L. Lapierre, ''Robust diving control of an AUV,'' *Ocean Eng.*, vol. 36, no. 1, pp. 92–104, 2009.
[10] R. Cui, X. Zhang, and D. Cui, ''Adaptive sliding-mode attitude control for autonomous underwater vehicles with input nonlinearities,'' *Ocean Eng.*, vol. 123, pp. 45–54, Sep. 2016.
[11] H. Joe, M. Kim, and S.-C. Yu, ''Second-order sliding-mode controller for autonomous underwater vehicle in the presence of unknown disturbances,'' *Nonlinear Dyn.*, vol. 78, no. 1, pp. 183–196, Oct. 2014.
[12] F. Rezazadegan, K. Shojaei, F. Sheikholeslam, and A. Chatraei, ''A novel approach to 6-DOF adaptive trajectory tracking control of an AUV in the presence of parameter uncertainties,'' *Ocean Eng.*, vol. 107, pp. 246–258, Oct. 2015.
[13] L. Qiao and W. Zhang, ''Adaptive non-singular integral terminal sliding mode tracking control for autonomous underwater vehicles,'' *IET Control Theory Appl.*, vol. 11, no. 8, pp. 1293–1306, May 2017.
[14] D. Maalouf, A. Chemori, and V. Creuze, ''L_1 adaptive depth and pitch control of an underwater vehicle with real-time experiments,'' *Ocean Eng.*, vol. 98, pp. 66–77, Apr. 2015.
[15] A. J. Healey and D. Lienard, ''Multivariable sliding mode control for autonomous diving and steering of unmanned underwater vehicles,'' *IEEE J. Ocean. Eng.*, vol. 18, no. 3, pp. 327–339, Jul. 1993.
[16] M. Kim, H. Joe, J. Kim, and S.-C. Yu, ''Integral sliding mode controller for precise manoeuvring of autonomous underwater vehicle in the presence of unknown environmental disturbances,'' *Int. J. Control*, vol. 88, no. 10, pp. 2055–2065, 2015.
[17] K. Isa, M. R. Arshad, and S. Ishak, ''A hybrid-driven underwater glider model, hydrodynamics estimation, and an analysis of the motion control,'' *Ocean Eng.*, vol. 81, pp. 111–129, May 2014.
[18] H. Akçakaya and L. G. Sümer, ''Robust control of variable speed autonomous underwater vehicle,'' *Adv. Robot.*, vol. 28, no. 9, pp. 601–611, 2014.
[19] C. Shen, B. Buckham, and Y. Shi, ''Modified C/GMRES algorithm for fast nonlinear model predictive tracking control of AUVs,'' *IEEE Trans. Control Syst. Tech.*, vol. 25, no. 5, pp. 1896–1904, Sep. 2017.

[20] W. Naeem, R. Sutton, J. Chudley, F. R. Dalgleish, and S. Tetlow, "An online genetic algorithm based model predictive control autopilot design with experimental verification," *Int. J. Control*, vol. 78, no. 14, pp. 1076–1090, 2005.
[21] N. Syahroni, Y. B. Seo, and J. W. Choi, "Open control platform implementation for autonomous underwater vehicle," in *Proc. Annu. Conf. SICE*, Takamatsu, Japan, Sep. 2007, pp. 2042–2047.
[22] Q. Chen, T. Chen, and Y. Zhang, "Research of GA-based PID for AUV motion control," in *Proc. Int. Conf. Mechatronics Autom. (ICMA)*, Changchun, China, Aug. 2009, pp. 4446–4451.
[23] Q. Zhang, "A hierarchical global path planning approach for AUV based on genetic algorithm," in *Proc. IEEE Int. Conf. Mechatronics Autom.*, Luoyang, China, Jun. 2006, pp. 1745–1750.
[24] J.-H. Li, B.-H. Jun, P.-M. Lee, and S.-W. Hong, "A hierarchical real-time control architecture for a semi-autonomous underwater vehicle," *Ocean Eng.*, vol. 32, no. 13, pp. 1631–1641, Sep. 2005.
[25] Z.-Z. Chu and M.-J. Zhang, "Fault reconstruction of thruster for autonomous underwater vehicle based on terminal sliding mode observer," *Ocean Eng.*, vol. 88, pp. 426–434, Sep. 2014.
[26] M. Chyba, S. Grammatico, V. T. Huynh, J. Marriott, B. Piccoli, and R. N. Smith, "Reducing actuator switchings for motion control of autonomous underwater vehicles," in *Proc. Amer. Control Conf.*, Jun. 2013, pp. 1406–1411.
[27] R. Rout, B. Subudhi, and S. Mahapatra, "Development of a NARMAX based constraint-adaptive heading controller for an autonomous underwater vehicle," in *Proc. OCEANS*, Shanghai, China, Apr. 2016, pp. 1–5.
[28] Y. S. Song and M. R. Arshad, "Sliding mode depth control of a hovering autonomous underwater vehicle," in *Proc. IEEE Int. Conf. Control Syst., Comput. Eng. (ICCSCE)*, Nov. 2015, pp. 435–440.
[29] J. Richalet and K. E. O'Donovan, "Donal with a foreword by Astrom," in *Predictive Functional Control: Principles and Industrial Applications*. Springer, 2009.
[30] C. Conte, C. N. Jones, M. Morari, and M. N. Zeilinger, "Distributed synthesis and stability of cooperative distributed model predictive control for linear systems," *Automatica*, vol. 69, pp. 117–125, Jul. 2016.
[31] M. Korda and C. N. Jones, "Stability and performance verification of optimization-based controllers," *Automatica*, vol. 78, pp. 34–45, Apr. 2017.
[32] H. C. La, A. Potschka, and H. G. Bock, "Partial stability for nonlinear model predictive control," *Automatica*, vol. 78, pp. 14–19, Apr. 2017.
[33] R. De Keyser, C. Copot, A. Hernandez, and C. Ionescu, "Discrete-time internal model control with disturbance and vibration rejection," *J. Vibrat. Control*, vol. 23, no. 1, pp. 3–15, Jan. 2017.
[34] M. M. G. Plessen and A. Bemporad, "Reference trajectory planning under constraints and path tracking using linear time-varying model predictive control for agricultural machines," *Biosyst. Eng.*, vol. 153, pp. 28–41, Jan. 2017.
[35] F. Fele, J. M. Maestre, and E. F. Camacho, "Coalitional control: Cooperative game theory and control," *IEEE Control Syst.*, vol. 37, no. 1, pp. 53–69, Feb. 2017.
[36] A. Zhakatayev, M. Rubagotti, and H. A. Varol, "Closed-loop control of variable stiffness actuated robots via nonlinear model predictive control," *IEEE Access*, vol. 3, pp. 235–248, 2015.
[37] A. A. Amanatiadis *et al.*, "A multi-objective exploration strategy for mobile robots under operational constraints," *IEEE Access*, vol. 1, pp. 691–702, 2013.
[38] P. Maurya, A. P. Aguiar, and A. Pascoal, "Marine vehicle path following using inner-outer loop control," *IFAC Proc. Vol.*, vol. 42, no. 18, pp. 38–43, 2009.
[39] J. González, S. Gomáriz, C. Batlle, and C. Galarza, "Fuzzy controller for the yaw and velocity control of the Guanay II AUV," in *Proc. IFAC Workshop Navigat., Guid. Control Underwater Vehicles (NGCUV)*, May 2015, vol. 48. no. 2, pp. 268–273.
[40] M. Sugeno, *Industrial Applications of Fuzzy Control*. Amsterdam, The Netherlands: Elsevier, 1985.
[41] T. I. Fossen, *Guidance and Control of Ocean Vehicles*. Hoboken, NJ, USA: Wiley, 1994.
[42] J. González-Agudelo, I. Masmitjà, S. Gomáriz-Castro, C. Batlle, D. Sarrià-Gandul, and J. del-Río-Fernández, "Mathematical model of the Guanay II AUV," in *Proc. MTS/IEEE OCEANS-Bergen*, Jun. 2013, pp. 1–6.
[43] J. G. Agudelo, "Contribution to the model and navigation control of autonomous underwater vehicle," Ph.D. dissertation, Barcelona East School Eng., Dept. Electron. Eng., Polytech. Univ. Catalonia, Barcelona, Spain, Jul. 2015.
[44] SNAME, *Nomenclature for Treating the Motion of a Submerged Body Through a Fluid*. New York, NY, USA: Society of Naval Architects and Marine Engineers, 1950, pp. 1–5.
[45] D. Zumoffen, L. Garyulo, M. Basualdo, and L. Jiménez, "Predictive functional control applied to multicomponent batch distillation column," *Comput. Aided Chem. Eng.*, vol. 20, pp. 1465–1470, Jun. 2007.
[46] S. Štampar, S. Sokolič, and G. Karer, "Predictive functional control of temperature in a pharmaceutical hybrid nonlinear batch reactor," *Chem. Ind. Chem. Eng. Quart.*, vol. 19, no. 4, pp. 573–582, 2013.
[47] R. Zhang and F. Gao, "Multivariable decoupling predictive functional control with non-zero–pole cancellation and state weighting: Application on chamber pressure in a coke furnace," *Chem. Eng. Sci.*, vol. 94, pp. 30–43, May 2013.
[48] J. Richalet and D. O'Donovan, "Elementary predictive functional control: A tutorial," in *Proc. Int. Symp. Adv. Control Ind. Process. (ADCONIP)*, May 2011, pp. 306–313.
[49] J. A. Rossiter, R. Haber, and K. Zabet, "Pole-placement predictive functional control for over-damped systems with real poles," *ISA Trans.*, vol. 61, pp. 229–239, Mar. 2016.
[50] M. T. Khadir and J. V. Ringwood, "Extension of first order predictive functional controllers to handle higher order internal models," *Int. J. Appl. Math. Comput. Sci.*, vol. 18, no. 2, pp. 229–239, 2008.
[51] C. Su, H. Shi, P. Li, and J. Cao, "Advanced control in a delayed coking furnace," *Meas. Control*, vol. 48, no. 2, pp. 54–59, 2015.
[52] W. Xu, J. Zhang, and R. Zhang, "Application of multi-model switching predictive functional control on the temperature system of an electric heating furnace," *ISA Trans.*, vol. 68, pp. 287–292, May 2017.
[53] R. Haber, U. Schmitz, and K. Zabet, "Implementation of PFC (predictive functional control) in a petrochemical plant," *IFAC Proc. Vol.*, vol. 19, no. 3, pp. 5333–5338, 2014.

WILMAN ALONSO PINEDA MUÑOZ was born in Bolívar-Cauca, Colombia, in 1975. He received the B.S. degree in electronic engineering from the Universidad Pedagógica y Tecnológica de Colombia in 2002 and the M.S. degree in computer science from the Universidad Autónoma de Bucaramanga, Colombia, in charter with the Instituto Tecnológico y de Estudios Superiores de Monterrey, Monterrey, Mexico, in 2006. He is currently pursuing the Ph.D. degree in electronic engineering with the Universidad de Los Andes, Bogotá, Colombia. He has been evolved in the Industria Militar de Colombia and the Instituto Colombiano de Petróleos conducting research. From 2002 to 2006, he was an Assistant Professor with the System Engineering and Electronic Technology Faculty, Fundación Universitaria Juan de Castellanos, Tunja, Colombia. Since 2007, he has been an Assistant Professor of electromechanical engineering. He is currently a Co-Founder and the Director of the GENTE Research Group, Universidad Pedagógica y Tecnológica de Colombia. Since 2014, he has been a member of the GIAP Research Group, Universidad de Los Andes. His research interests include computer science, automation and control; spatially, autonomous vehicles, guidance systems, control and navigation systems, and predictive control. He was a recipient of the scholarship for excellence granted by Colciencias in 2012.

ALAIN GAUTHIER SELLIER was born in Annonay, France, in 1951. He received the B.S. degree in electrical engineering from the University of Grenoble in 1972, and the master's and Ph.D. degrees in automatic from the Grenoble Institute of Technology, France, in 1974 and 1978, respectively. He was a Researcher in the research center of the Brown Boveri Group in Paris and Lyon and participated in the development of controllers for electrical generation of nuclear power station and in the modeling and control of synchronous machines. He has been an associate with the Universidad de Los Andes since 1983. He coordinated scientific and technical cooperation programs with the French Government from 1985 to 2003. He was a National Coordinator of the PCP Program in industrial automation from 1994 to 2003, a Coordinator for Latin America of the Alfa Air network with the European Union from 1997 to 1999, as well as a Vice-President, a Founding Member, and a Honorary Member of the Colombian Association of Automatic. He was a Coordinator of the master's degree in electrical engineering, a Director of the Department of Electrical and Electronic Engineering, a Post-Graduate and Research Director of the Faculty of Engineering, as well as the Dean of this Faculty from 2005 to 2013. In this period, among his most important challenges was the improvement of the undergraduate Saber Pro exam, duty in which he succeeded in maintaining the accreditations of the programs undergraduate and master's, implementing the quality system, as well as achieving ABET Accreditation. For this work, he received a congratulatory motion from the Superior Council of the University of the Andes. He was the coordinator of the Doctoral and Master National Commission (National Education Ministry Colombia) from 2001 to 2003 (part time). He has authored more than 50 articles in congresses or magazines. His main research topics include the identification and control of multivariate systems, the control of hybrid systems, optimal control, and the application of control theory. Precisely for his contributions in this area, the IEEE CSS branch (IEEE Control System Society section Colombia) created the Alain Gauthier award, which is granted that is awarded to a leading engineer in the control area who has made significant contributions in education and research, or in projects that have led to important industrial collaboration. He received the first one in 2011.

SPARTACUS GOMÀRIZ CASTRO received the bachelor's, M.Sc., and Ph.D. degrees in telecommunication engineering from the Universitat Politècnica de Catalunya (UPC), Barcelona, Spain, in 1990, 1995, and 2003, respectively. He is currently an Associate Professor with the Department of Electronic Engineering, UPC, and a member of the research group remote acquisition systems and data processing (SARTI). From 1990 to 2009, he was a Teaching Assistant with the Vilanova i la Geltrù School of Engineering, and from 2010 to 2015 with the Escola Universitària d'Enginyeria Tècnica Industrial de Barcelona. In 2016, he joined the staff of the Barcelona East School of Engineering, UPC. His research interests include linear and nonlinear control theory, gain scheduled control, fuzzy control, design of navigation, guidance, and control systems for underwater vehicles. He has authored three books, 44 journal articles, over 92 presentations of his work at congresses, and three theses. He has been involved in 18 national and international competitive research projects. He is currently a member of the following societies: the IEEE Oceanic Engineering Society and the Spanish Committee of Automation of the International Federation of Automatic Control. Besides, he is involved in Spanish Research Networks: Marine Robotics and Automation and Instrumentation and Applied Technology for the Study, Characterization, and Sustainable Exploration of Marine Environment (MarInTech).